

INFRARED SENSING TECHNIQUES

FOR ADAPTIVE ROBOTIC WELDING

T. T. Lin, K. Groom, N. H. Madsen and B. A. Chin

Department of Mechanical Engineering,
Auburn University, Auburn, AL 36849

CONF-860132--4

DE86 013277

Abstract

The objective of this research is to investigate the feasibility of using infrared sensors to monitor the welding process. Data were gathered using an infrared camera which was trained on the molten metal pool during the welding operation. Several types of process perturbations which result in weld defects were then intentionally induced and the resulting thermal images monitored. Gas tungsten arc using AC and DC currents and gas metal arc welding processes were investigated using steel, aluminum and stainless steel plate materials. The thermal images obtained in the three materials and different welding processes revealed nearly identical patterns for the same induced process perturbation. Based upon these results, infrared thermography is a method which may be very applicable to automation of the welding process.

DISCLAIMER

This report was prepared as an account of work sponsored by an agency of the United States Government. Neither the United States Government nor any agency thereof, nor any of their employees, makes any warranty, express or implied, or assumes any legal liability or responsibility for the accuracy, completeness, or usefulness of any information, apparatus, product, or process disclosed, or represents that its use would not infringe privately owned rights. Reference herein to any specific commercial product, process, or service by trade name, trademark, manufacturer, or otherwise does not necessarily constitute or imply its endorsement, recommendation, or favoring by the United States Government or any agency thereof. The views and opinions of authors expressed herein do not necessarily state or reflect those of the United States Government or any agency thereof.

MASTER

DISTRIBUTION OF THIS DOCUMENT IS UNLIMITED

FC4B

Introduction

Automatic welding is commonplace in industry today. However, most, if not all, involves preprogramming for performance of a repetitive task. These systems are incapable of correcting for perturbations which arise during the welding process. Control of the welding process requires the identification and monitoring of perturbations in a wide variety of parameters. The varied nature of these parameters and the large number of variables involved have thwarted previous attempts at closed loop control of the welding process. The sensor(s) employed by a control system need to meet rather strenuous requirements. First and foremost of these is that such a sensor must be able to identify and discriminate between perturbations that might affect the quality of the weld, including such geometrical perturbations as a change of direction in the seam between the parts being welded, gaps in the seam or a misalignment of the parts being welded. The sensor should also be able to locate and identify contaminants and impurities in the weld puddle and ahead of it while monitoring the extent of the heat-affected zone and the cooling rate of the metal. The sensor(s) should, additionally, be able to perform these tasks in a time frame that is consistent with automatic control of the welding process. This paper presents results that could aid in the assembly of such a controlled welding system.

The high temperatures associated with metal arc welding and the appropriate thermophysical properties (primarily thermal diffusivity) of the parts to be welded cause very strong spatial temperature gradients (of over 10^6 C/m) in the vicinity of the weld pool surface. Modern infrared thermography equipment permits rapid sensing of these gradients with a high degree of accuracy. During an ideal weld these gradients should show repeatable and regular patterns. However, imperfections should cause a discernable change in the thermal profiles. Based on this hypothesis, experiments were carried out to determine the quality and magnitude of the thermal changes as a function of specific induced weld flaws, arc or plate misalignment, penetration, and contamination.

Specific weld defects were intentionally induced into an arc welding process and the resulting surface isotherms were observed using a scanning infrared camera for both stationary and moving arcs. Each weld defect produced a distinctively different distribution of the surface temperature. The infrared camera is capable of monitoring arc position relative to the seam and can be used to identify plate geometry defects such as plate gaps and offset. Changes in the patterns of surface isotherms in front of a moving arc are directly related to the presence of impurities and obstruction. Defects as small as 1/32" in diameter can be observed in the molten metal pool prior to solidification.

Work during the last 18 months has concentrated on determining: 1. the applicability of the infrared sensing technique to the welding of different metals (whether the same thermal patterns associated with welding process variations appear in materials with different thermal conductivity, emissivity, melting point, and properties, i.e. in steel, aluminum and stainless steel); 2. the applicability of the infrared sensing technique to monitoring different welding processes (Gas Tungsten Arc and Gas Metal Arc Processes); and 3. the construction of the interface and computer software for real time feedback control. Each of these items will be discussed in one of the following sections.

experimental procedure

Experiments were conducted on plates of AISI 1040 steel, 5454 Aluminum, 6061 Aluminum and AISI 304 stainless steel. Three standard plate thicknesses were used (0.1875"; 0.25" and 0.375") with all plates being 12" x 6" in size. The edges of the plates to be joined were milled for a precise fit. Plate surfaces near edges to be joined were cleaned prior to welding. These plates were gas tungsten arc (GTA) or gas metal arc (GMA) welded in a butt joint configuration. GTA welding was performed with a Miller Syncrowave 500 AC/DC power source and a water-cooled torch. A 0.125" (3.175 mm) pure tungsten electrode was used for Al and a 2% thoriated tungsten electrode used for steel. Electrode stickout past the gas cup and arc length were maintained at 0.125". The electrode tip was ball-shaped for welding aluminum and conical for steel. The torch was mounted to Heath Engineering Co. ESAB X-Y positioning table (Model #ICD/600-MODFD) which is connected to a Hewlett Packard 9836 computer, shown in Figure 1 with associated acquisition and control interfaces. GTA arc currents were varied between 30 and 200 A at 30 VAC and 28 VDC with an Argon shielding gas. GMA welding was performed with an ESAB-LAH315 pulse arc power source and ESAB A10-MEC44 wire feed unit. Shielding gas was a 95% Ar-5% CO composition for welding steel. Arc currents between 150 and 300 A at 30 VDC were used. The current was measured using a Columbia Electric Mfg. Co. tong test (Model AX) clampon ammeter with a scale of 0-300 amperes.

An infrared scanning camera was positioned for front side viewing of the plate surface during welding. Infrared imaging equipment manufactured by Inframetrics Co. (Model 525) and AGA (Model 780) were used. This equipment consists of a single waveband (8-12 microns) infrared scanner (IR detector), infrared signal processor (control/electronics unit), color enhancement processor (colorizer), power supply/charger, color video monitor and video cassette recorder. The instruments are capable of measuring temperatures from -20 to 2500°C (-4 to 4532°F) with a temperature resolution of $\pm 0.2^\circ\text{C}$.

The operation of this infrared equipment is as follows. First the scanner detects heat at the surface by capturing thermal radiation emitted as infrared electromagnetic waves. This scanner includes an electro-optical transducer that converts infrared radiation to an electrical signal. Such information is compiled and amplified by an infrared signal processor, which generates a video-compatible signal that produces thermograms on a video monitor. The color monitor is used to display the thermograms that show temperature fields as a gradation from black to white or from cold to hot. Finally, all thermal images were recorded and stored on a Panasonic video cassette recorder for future analysis. The thermograms can then be photographed with a 35 mm camera after welding is complete. Direct transfer of infrared thermography data to an HP9836 computer is performed using a custom designed smart interface which is capable of analyzing 3-5 (100 x 100) matrices of data every second.

Identification of Weld Process Perturbations in Steel, Aluminum, and Stainless Steel

To investigate the applicability of the infrared sensing technique to different materials, a set of experiments were conducted using steel (AISI 1040), aluminum (5054, 6061) and stainless steel (AISI 304) plates. These materials were selected to cover the range of material welding variables (thermal conductivity, melting point, emissivity, etc.) that might

Chir

3

13

reasonably be encountered during 90% of all welding operations. For instance the melting point of Al is approximately 660°C while that of stainless steel is 1550°C . Additionally the thermal conductivity of aluminum, steel, and stainless steel are 0.16, 0.048, and 0.015 watts/ $\text{mm}^{\circ}\text{C}$ respectively. In other words, an order of magnitude difference exists between the thermal conductivities.

Experiments were conducted using both AC and DC gas tungsten arc welding in aluminum and DC gas tungsten arc welding in steel and stainless steel. Both frontside and backside infrared camera positions were investigated. Figure 2 shows the infrared images for a stationary arc placed within 0.01" of the seam center of the aluminum and steel plates. In the top photographs which are two dimensional surface temperature distributions, different color bands of the images represent different temperature ranges. For the steel the darker shades represent cold temperatures and the lighter shades represent hotter temperatures. A reverse color assignment has been used to separate Al infrared images from steel images (hot = dark, cold = light). At the bottom of each thermal image photograph, a color bar shows the color assignment to regions of temperature ranging from coolest to hottest.

Notice that the thermal images are both symmetrical indicating that the arc is on seam. The patterns are nearly identical despite the fact that temperatures between 25 and 650°C are being monitored in the Al and temperatures from 25 to 1600°C are being monitored in the steel. Located below the thermograms for steel and aluminum are temperature versus distance scans across the center of the two dimensional images in Figure 2. The dotted horizontal line indicates position of the temperature versus distance profile. Again the temperature distribution is symmetrical indicating positioning of the arc over the weld center.

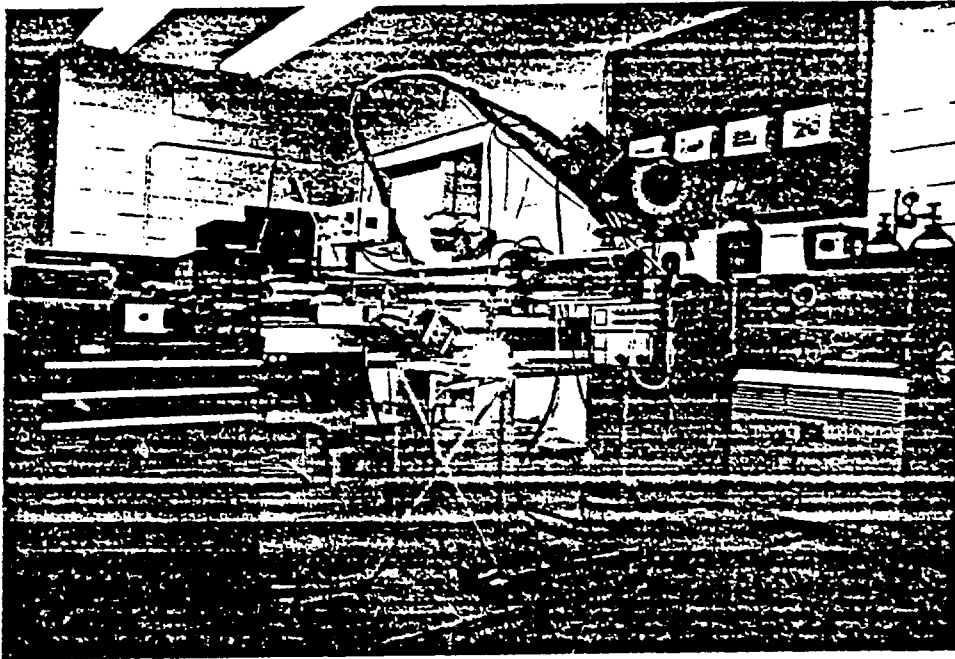


Figure 1: Equipment used in arc welding and position of infrared camera for front side measurements.

Chin

↑

13

Experimenta Procedure

Experiments were conducted on plates of AISI 1040 steel, 5454 Aluminum, 6061 Aluminum and AISI 304 stainless steel. Three standard plate thicknesses were used (0.1875"; 0.25" and 0.375") with all plates being 12" x 6" in size. The edges of the plates to be joined were milled for a precise fit. Plate surfaces near edges to be joined were cleaned prior to welding. These plates were gas tungsten arc (GTA) or gas metal arc (GMA) welded in a butt joint configuration. GTA welding was performed with a Miller Syncrowave 500 AC/DC power source and a water-cooled torch. A 0.125" (3.175 mm) pure tungsten electrode was used for Al and a 2% thoriated tungsten electrode used for steel. Electrode stickout past the gas cup and arc length were maintained at 0.125". The electrode tip was ball-shaped for welding aluminum and conical for steel. The torch was mounted to Heath Engineering Co. ESAB X-Y positioning table (Model #ICD/600-MODFD) which is connected to a Hewlett Packard 9836 computer, shown in Figure 1 with associated acquisition and control interfaces. GTA arc currents were varied between 30 and 200 A at 30 VAC and 28 VDC with an Argon shielding gas. GMA welding was performed with an ESAB-LAH315 pulse arc power source and ESAB A10-MEC44 wire feed unit. Shielding gas was a 95% Ar-5% CO composition for welding steel. Arc currents between 150 and 300 A at 30 VDC were used. The current was measured using a Columbia Electric Mfg. Co. tong test (Model AX) clamp ammeter with a scale of 0-300 amperes.

An infrared scanning camera was positioned for front side viewing of the plate surface during welding. Infrared imaging equipment manufactured by Inframetrics Co. (Model 525) and AGA (Model 780) were used. This equipment consists of a single waveband (8-12 microns) infrared scanner (IR detector), infrared signal processor (control/electronics unit), color enhancement processor (colorizer), power supply/charger, color video monitor and video cassette recorder. The instruments are capable of measuring temperatures from -20 to 2500°C (-4 to 4532°F) with a temperature resolution of + 0.2°C.

The operation of this infrared equipment is as follows. First the scanner detects heat at the surface by capturing thermal radiation emitted as infrared electromagnetic waves. This scanner includes an electro-optical transducer that converts infrared radiation to an electrical signal. Such information is compiled and amplified by an infrared signal processor, which generates a video-compatible signal that produces thermograms on a video monitor. The color monitor is used to display the thermograms that show temperature fields as a gradation from black to white or from cold to hot. Finally, all thermal images were recorded and stored on a Panasonic video cassette recorder for future analysis. The thermograms can then be photographed with a 35 mm camera after welding is complete. Direct transfer of infrared thermography data to an HP9836 computer is performed using a custom designed smart interface which is capable of analyzing 3-5 (100 x 100) matrices of data every second.

Identification of Weld Process Perturbations in Steel, Aluminum, and Stainless Steel

To investigate the applicability of the infrared sensing technique to different materials, a set of experiments were conducted using steel (AISI 1040), aluminum (5054, 6061) and stainless steel (AISI 304) plates. These materials were selected to cover the range of material welding variables (thermal conductivity, melting point, emissivity, etc.) that might

Chir

3

13

ARC POSITION - ON SEAM

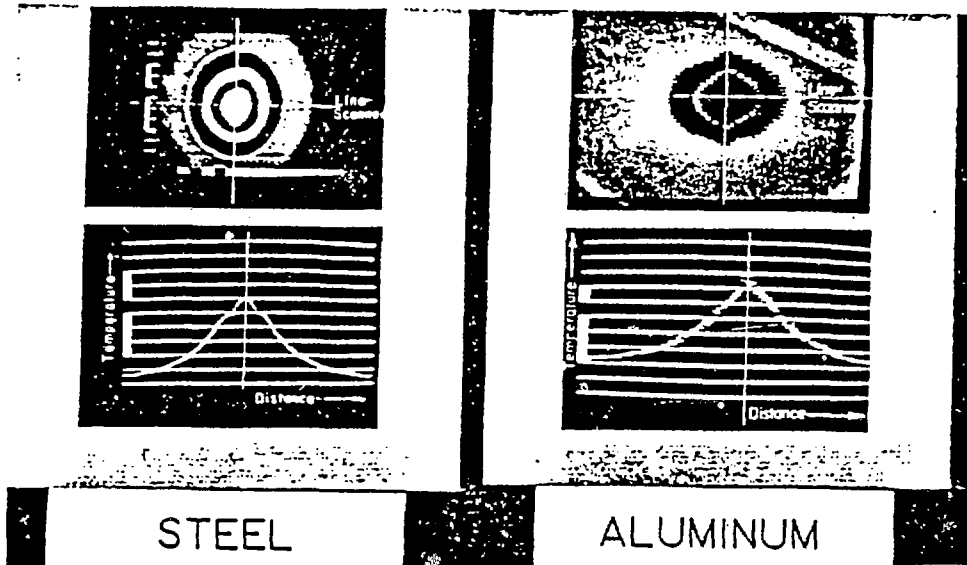


Figure 2: Stationary Arc in Aluminum and Steel. Arc placed within 0.01" of seam. Top photographs are two dimensional temperature distributions of plate surfaces during welding. Vertical solid white line is superimposed on photograph showing seam position. Bottom photographs are plots of temperature versus distance of dashed horizontal line of top photographs. Inflection points in temperature versus distance curves indicate molten metal-solid metal interface.

ARC POSITION - OFF SEAM

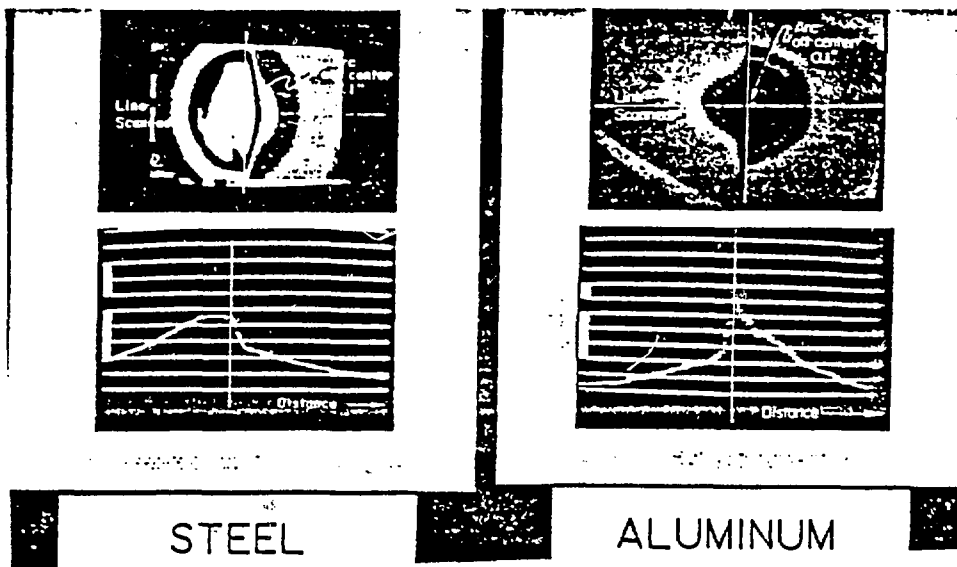


Figure 3: Stationary Arc in Aluminum and Steel. Arc placed 0.1" off seam center. Note asymmetry in both two dimensional temperature distributions and line scans.

Chin

5

13

An ancillary objective of this research effort was to determine the feasibility of CAD/CAM integrated welding. The practicality of controlling a welding robot based on welding design specifications was evaluated. The equipment included an ESAB LAH-315-P GMAW welding machine. The welding gun was mounted on a two axis positioning table and moved using two electric motors. The electric motors were conventionally controlled using an optical tracer. In this mode a weld path could be produced from a line drawing. The CAD/CAM package was developed on a Hewlett Packard 9836 computer. Peripherals including a digitizing tablet, plotter and data acquisition/control unit were available. The HP3497A data acquisition control unit was equipped with dual digital to analog converters, a realtime clock, and an actuator/digital output card. After the initial work, three dimensional movement capabilities and position sensors were added to the system. The digital to analog converters were used to generate control voltages for the electric motors. A relationship between control voltage and steady state translation speed was developed. System mass and damping factors were determined for use during transient conditions. Welding machine power was controlled using the relay actuator board. With this configuration the use of the optical tracer for control could be replaced by the computer. The path to be welded was defined using the digitizing tablet, welding speeds and welding on/off times were defined at the computer. With this system welds equal to or superior in quality to those generated using the optical tracer were produced. The advantage of being able to continuously vary welding speed produced significant improvements in weld quality at points where weld path radii of curvature were small. Problems with "losing" the path were eliminated. The first effort essentially emulated existing control techniques, except replaced teaching the robot with tracing the welding path on a digitizer. Even this offers some advantages, including programming the welder from part drawings.

The linkage of the infrared sensing system, data transfer interface, computer and manipulator control has been completed. Efforts are currently underway to demonstrate controlled feedback welding using infrared thermography.

CONCLUSIONS

The following conclusions resulted from this investigation.

- Infrared thermography can accurately monitor temperature plate distributions in aluminum, steel and stainless steel during the welding process.
- Infrared sensing systems are capable of detecting arc misalignment, plate mismatch, surface contamination and geometric defects such as plate gap and plate offset in a wide variety of materials.
- Thermal distributions seen in the welding of aluminum and stainless steel are very similar to those measured in steel. Only the magnitude of the thermal distributions varied due to thermal conductivity and melting point differences.
- Infrared sensors are applicable to monitoring AC/DC gas tungsten arc welding and gas metal arc welding operations.
- An intelligent real-time video interface has been developed to transfer information from the infrared camera to the computer at a speed consistent with on-line control.

Chin

To date, manufacturing processes involving welding have not benefited from this integration of design and manufacture. In environments where welding robots can be used, these robots are programmed after the parts to be welded have been manufactured. The path the welder is to follow is taught by setting up the pieces to be welded, and manipulating the robot through the required positions. These positions are stored in the robot memory for later use. The welding speed and other welding parameters are then programmed at the welding station through the use of a keyboard or some other interface. This procedure suffers from several disadvantages. It is difficult to assess the weldability of the parts until after their design and manufacture is complete. If the welder is not able to produce quality welds, significant time and effort has been wasted. If the parts used in programming the welder happen to be somewhat atypical, weld quality may not be maintained on the subsequent welds. Small design changes in the parts to be welded require that the robot be reprogrammed. Programming time and effort in training the robot is significant. This requires large numbers of the same part to justify the use of a robot. This time is spent telling the robot about decisions the designer has already made, and probably stored in a computer somewhere.

Many of the problems with welding robots described above could be overcome if the robot program could be generated during the weld process. During the design of the parts to be welded, the weld locations and parameters are specified. From these specifications, the sequence, speed, and weld parameters required of the robot can be determined. The control program for the robot can then be generated. If the robot cannot produce the required welds, the designer is alerted early in the process, so that the part design can be modified. The welder is programmed based on the typical part. Small design changes automatically produce the required welding robot program changes. The design process includes the generation of the welding program, eliminating robot programming time.

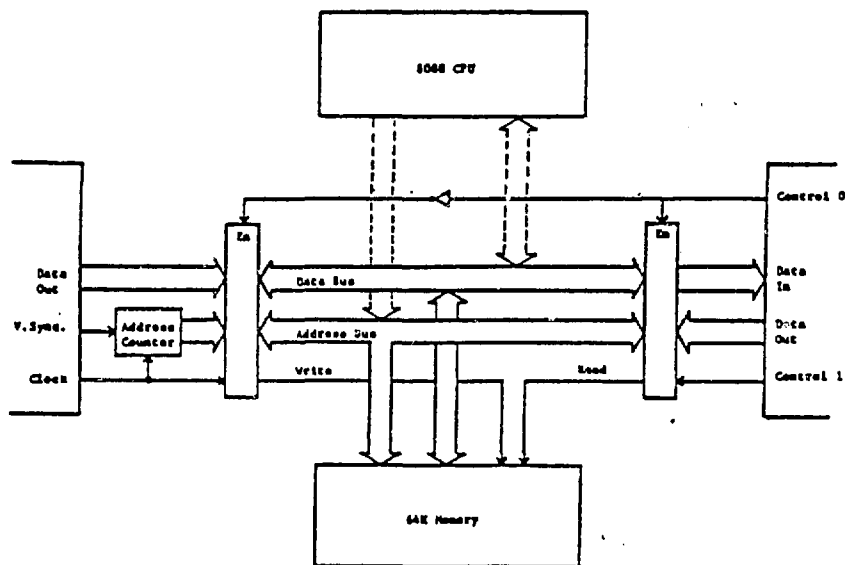


Figure 9: Schematic of Intelligent Interface for Transfer of Data from Inframetrics Camera to Control Computer.

Chir
12
13

thermal image is transferred. The horizontal sync line drops low and returns high once with each line of data transferred (328 clock pulses). Immediately after it returns high 33 clock pulses remain until data describing the thermal image will be transferred. The sync lines can be used with high speed counters to ensure capture of the desired 12.35 ms of data. The data lines can be tied to high speed memory data lines (for simplicity static 110 nanoseconds, 2K x 8 memory chips were used). The clock can be used to provide a data valid strobe to the memory chips and to increment an address counter for the memory. 48K x 8 bits of memory is required for one frame of data. A high speed Z-80 was chosen for the local microprocessor controller. It has a 64K x 8 bit address space, thus leaving 16K for ROM containing programs to interface with the HP9836 and for any RAM buffer required in the transfer. Although the chip count of the system could be reduced by the use of more complex and more expensive chips, simplicity and modularity were the basis of our design. Problems were identified easily and readily corrected without a massive redesign effort. A block diagram of the system is shown in Figure 9.

As the information transfer techniques were being developed concurrently, emphasis was placed on the development of open loop control techniques. In particular, control based directly on parameters specified in the design process was emphasized. Welding is an area where the integration of CAD/CAM promises many benefits. Many computer-aided design programs generate the numerical control code required to perform the appropriate manufacturing process. For example it is common to generate the control code for cutting tool movement from the design of the part to be cut. This ability is beneficial in several ways. During the design process a determination of the feasibility and probable quality of manufacture can be made, and the design modified appropriately. The completion of the design provides everything necessary to initiate the manufacturing process, producing a significant time saving.

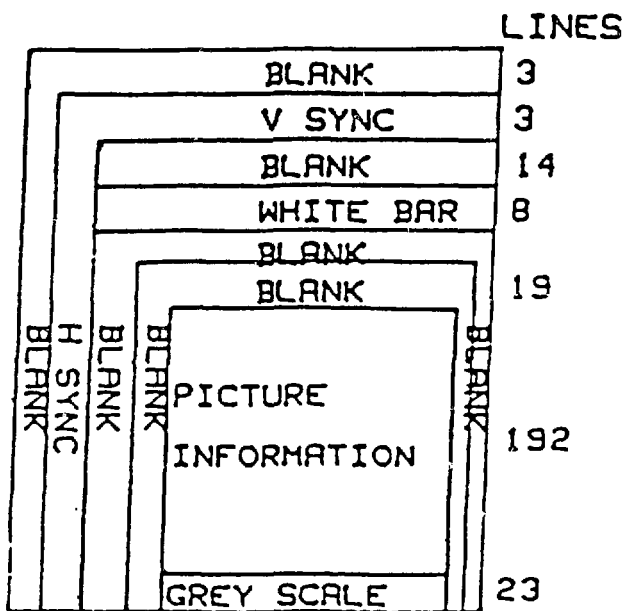


Figure 8: Timing Diagram for Information Output by Inframetrics camera.

Chin
11
13

Real-Time Control: Seam Tracking

Real time control of the welding process using infrared thermography depends upon efficient transfer of thermal image information to the computer, identification of the perturbation from the thermal image and issuing the proper correction sequence. To demonstrate that the above events can be accomplished in a time frame consistent with on-line control, the appropriate hardware for transfer of information to and from the computer has been fabricated along with the necessary software for control of arc position perturbations i.e., seam tracking. A description of the interface hardware follows.

Timely transfer of the information contained in the infrared image to the controlling computer is a critical issue in closed loop control of the welding process. The Inframetrics 525 imaging system used in this research provides an 8 bit parallel output at a 5.1 MHz clock rate (typical of a video system). Thus thermal sensitivity is 1 part in 256. Temperature data is available every 193.5 nanoseconds. The HP9836 computer system has a maximum transfer data of 0.930 MHz. (burst DMA) with 16 bits in parallel. Even transferring two temperatures at a time, direct communication is not possible. Although several commercially available units allow one to store a frame of video data for later use, there did not appear to be any available means for continuous high speed transfer of significant amount of information from a video system to a computer. In response to this situation we have developed an intelligent interface that will allow us to select what characteristics of the infrared image will be transferred to the controlling computer, transmit a significant amount of information each frame, and update these parameters on a frame by frame basis.

The timing of the information provided by the Inframetrics system is shown in Figure 8. The salient features of this timing diagram include the observations that a frame of information is transmitted every 262 (number of lines) $\times 328$ (clock pulses per line) $\times 1/5.1 \times 10^6$ (clock rate) seconds. Thus an entire infrared image is transferred every 16.85 ms (=60 frame/second). However of this 16.85 ms, only 12.35 ms (192 lines) is used to transfer temperature information. This represents 48000 8 bit bytes. The remaining 4.5 ms from the end of one frame to the beginning of the next provides a window for information transfer to the computer. The approach followed was to develop a memory buffer that would temporarily hold a frame's worth of temperatures, and to provide a local microprocessor that would use the 4.5 ms to transfer selected portions of the thermal image to the HP9836 computer. Using the burst DMA mode with the GPIO interface some 4185 words of 16 bits each could be transferred in that time. The frame buffer and microprocessor have been developed and are described in the following. Algorithms for selecting the most appropriate data to transfer have not been developed. Nor have algorithms for treating that data upon arrival at the Hewlett-Packard computer. It is also worth noting that for maximum simplicity our first design allows only mutually exclusive memory buffer access by the infrared imaging unit and the local microprocessor. Subsequent designs may permit more nearly concurrent usage if increased window time for the transfer is required.

The output from the Inframetrics 525 Thermal Imaging System contains 11 significant lines. These include 8 data lines, a clock line, the horizontal and vertical sync lines. The 5.1 MHz clock is high for approximately 135 nanoseconds every cycle. The data lines are valid from 10 nanoseconds before the clock goes high until 30 nanoseconds after it has returned low. The sync lines provide information regarding what portion of the thermal image is being transferred. The vertical sync lines drop low and return high once each frame. Immediately after it returns high, 41 lines of data must be transferred before the actual

Chin

10

13

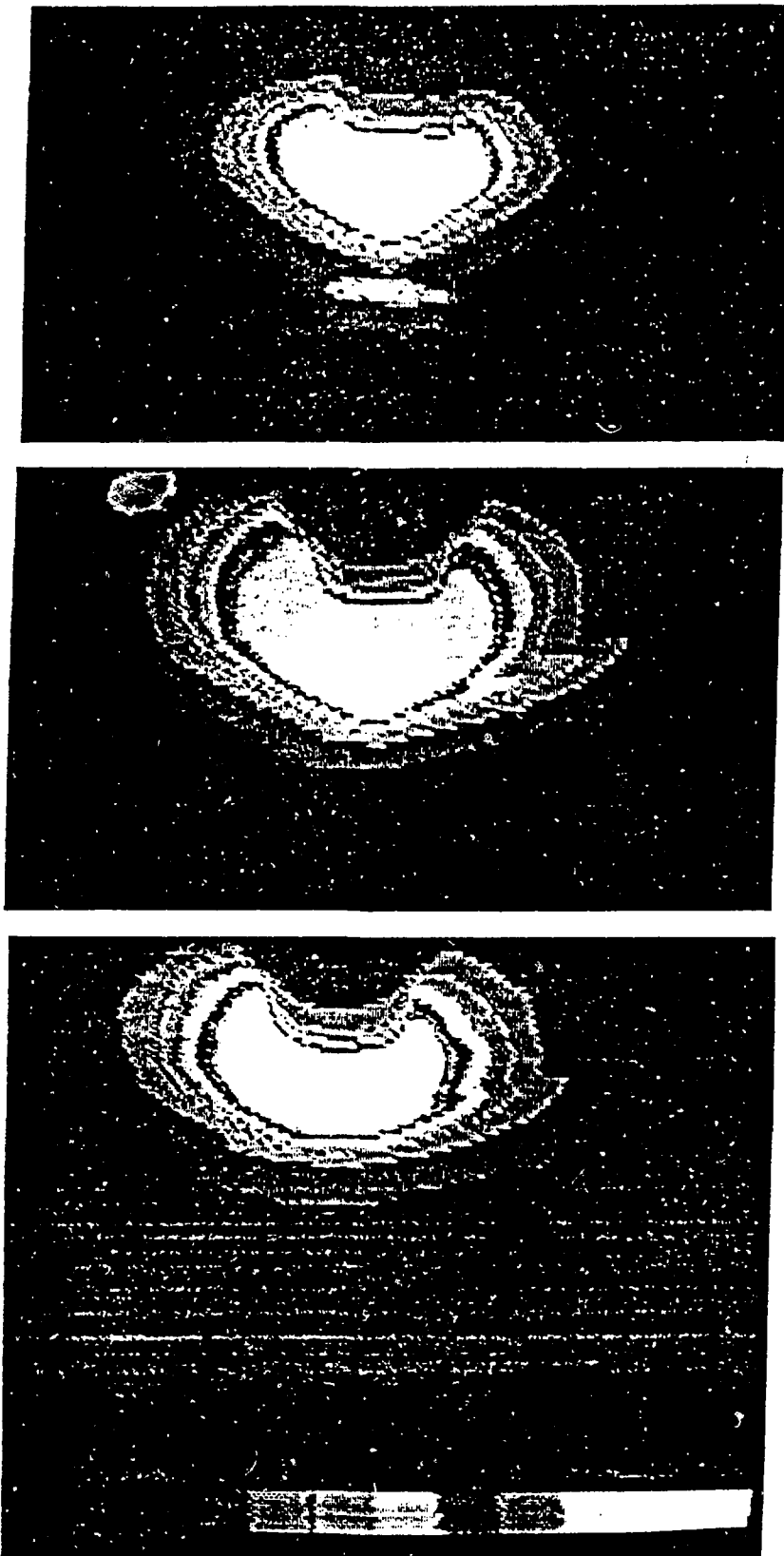


Figure 7: Identification of Lack of Fusion during GMA welding caused by aluminum oxide surface contamination of AISI 1040 steel. Sequential thermal images were taken:

- a. thermal image front encounters contamination
- b. molten pool front encounters contamination
- c. contamination extends through molten pool.

Chin

In the previous section, thermal images were presented for gas tungsten arc welding using both DC and AC current. The aluminum welding was conducted using DC and AC current while all steel images were produced using DC current. In both cases high frequency was used to start the welding operation. Proper grounding and electrical isolation were required to obtain images during the high frequency start.

The only influence that polarity and current form has on thermal pattern identification is in the noise level of the signals coming from the infrared camera. AC welding resulted in a higher noise level. Resolution of inflection points in temperature versus distance scans (indication of molten metal-solid metal interface) was sometimes masked by the higher noise level.

Experiments were also conducted using the gas metal arc welding process. Similar thermal patterns were obtained for all weld process perturbations investigated in steel using the GTA and GMA processes. Disturbances of the molten metal, although identifiable in thermal images did not influence the ability to see intentionally induced defects. It is necessary to fabricate a lens filter of Si-Ge to protect the camera from splatter. This caused a reduction in intensity of the image received, but did not change the thermal distribution.

Figure 7 shows a sequence of thermal images obtained during gas metal arc welding of AISI 1040 steel. The current used was 150 amp at 240 V which places the welding process in the dip mode of metal transfer. The torch is moving at a rate of 6" per minute towards the bottom of the page. The thermal images were taken at different points in time, prior to, during and after encountering surface contamination (0.001" thick Al₂O₃ painted on the plate) at a 45° angle with respect to the seam. The sequence of images clearly show the intersection of this surface contaminant with the forward edge of the thermal image, molten pool and passing the surface contaminant.

SURFACE CONTAMINATION

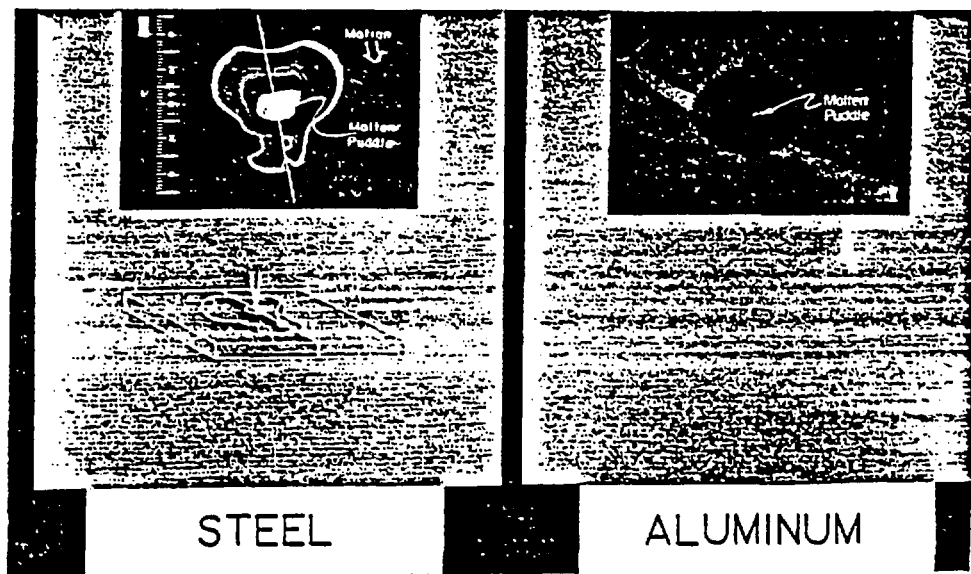


Figure 6: Surface Contamination Identification in Steel and Aluminum. In steel a 1/16" diameter aluminum oxide contaminant is identified by perturbations (white circle) in the thermal field. Schematic of experimental is shown in lower left hand photograph. A 1/8" diameter grease contaminant is identifiable in aluminum by the black dot in the top edge of the thermal pattern.

Chir

The results of these experiments show that similar thermal patterns to those identified in steel for intentionally induced process variations occur during the welding of aluminum and stainless steel. Only the magnitude of the temperature distributions is different principally because of the differences in the thermal conductivity of the material. Some initial difficulty was encountered from reflections of the hot torch and welding cup off the surface of the aluminum plates being welded. Reflections had not been encountered in the thermographic images measured in steel. The reflected image of the torch on the hot plate was eliminated by the placement of a water cooling jacket over the outside of the welding torch. Images produced in stainless steel were nearly identical to those found in the steel despite the differences in thermal conductivity.

Another difference that was encountered between experiments conducted in steel and aluminum was that the patterns in the thermal images tended to disappear at a shorter distance from the weld pool. This is the result of the higher thermal conductivity of aluminum. The principle effect that this has on the technique of using infrared thermography for monitoring the weld process is that instead of previewing upcoming events four to five inches ahead of the molten metal pool as was possible in steel, events are viewed one to two inches ahead of the molten pool. Thus infrared thermography appears to have applicability as a sensor across a wide range of materials. The effect of a lower thermal conductivity is to make the patterns corresponding to specific weld perturbations more distinguishable.

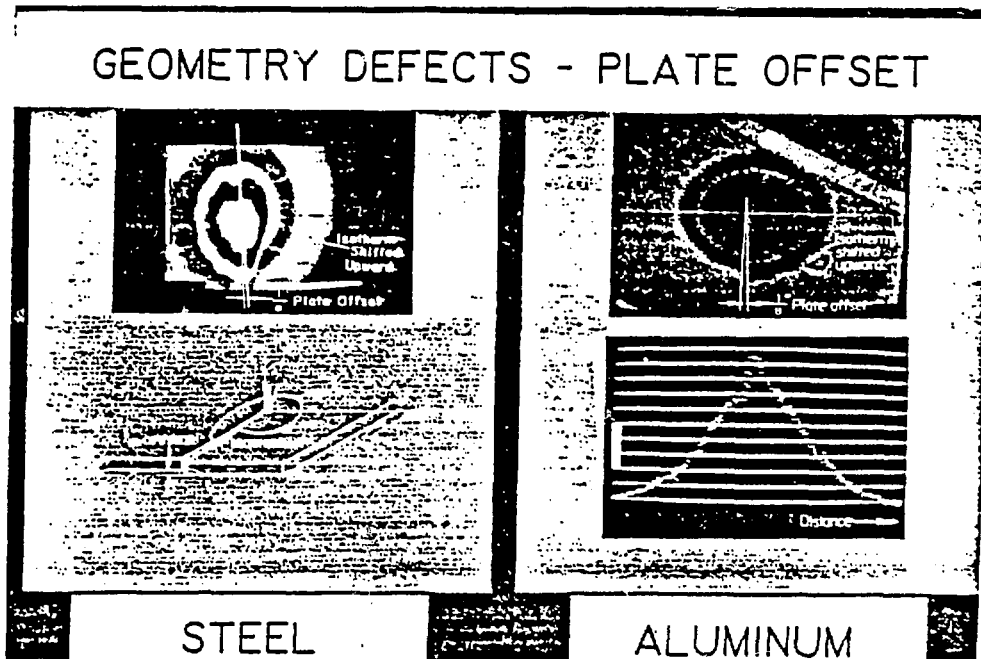


Figure 5: Plate mismatch identification in Steel and Aluminum. Schematic (bottom left) represents experimental setup. A snail shape thermal pattern is produced indicating one plate is closer to the arc. Line scan image in aluminum shows a dramatic drop in temperature across the seam.

Chin

Figure 3 shows the surface temperature distribution which results when the arc is positioned 0.1" off the seam center. The arc is displaced to the left of the seam for the aluminum and to the right for the steel. Again, images are shown for both steel and aluminum. The two dimensional thermal image of this figure is composed of half-moon shapes or portions of circles. This asymmetrical temperature distribution is caused by contact resistance at the seam. A marked difference in the thermal distribution symmetry for an arc placed on the seam versus a displacement at a distance of 0.1" off the center is seen by comparing images of Figure 2 and 3. The results obtained indicated that seam tracking may be based on the difference in radii of isothermal curves to the left and right of the seam.

In addition to seam tracking, the infrared sensor is capable of identifying surface contamination and geometrical variations such as joint gaps and mismatches in both Al and steel. Figure 4 shows the resulting two dimensional thermal distributions for seam gaps. The tapered gaps (1/16" at a distance 4" from the arc) in the seam cause a notch in the constant temperature lines corresponding to a decrease from the peak temperatures of the metal surrounding the gaps. Line scans of figure 4 show this drop in the temperature versus distance profile. The sensitivity of the sensor in identifying arc position is also seen in these Figures by the slight difference in peaks of the line scans.

Figure 5 shows the result of plate mismatch on the surface thermal distribution. Offsetting one end of one plate with respect to the other 0.125" (as shown in the skematic of Figure 5) causes a shift in the centers of the half-moon. In addition to seam tracking and detection of geometric plate variations, surface contamination also can be detected in the surface thermal field as shown in Figure 6. The contaminants are identified by circular abnormalities (white dot in steel, black dot in aluminum) in the thermal profiles.

GEOMETRY DEFECTS - PLATE GAPS

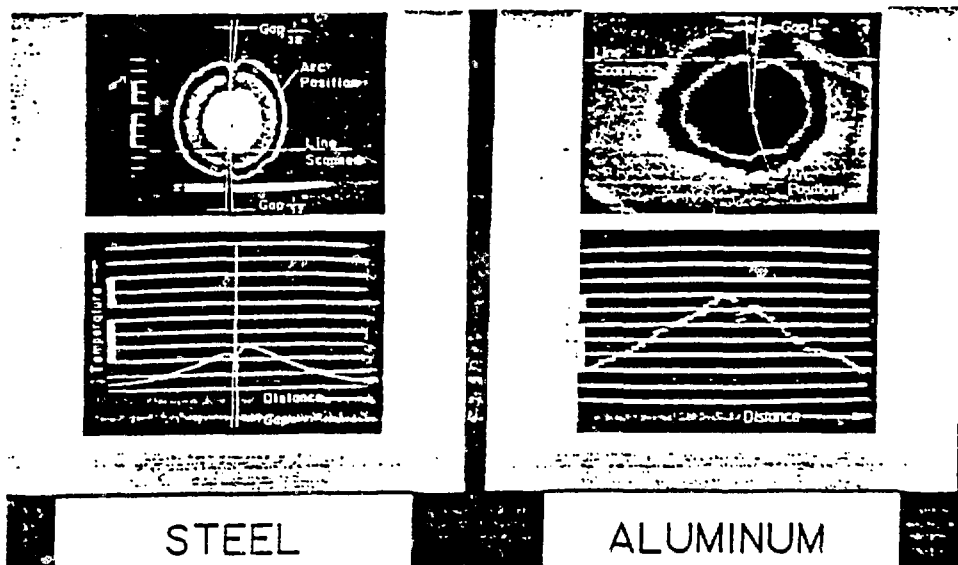


Figure 4: Seam Gap Identification in Aluminum and Steel. A tapered gap of 1/16" and 1/32" at 4" from weld pool center causes the isotherms to develop a notch. Differences in peak temperatures on sides of notches of temperature versus distance scans indicate arc is slightly off seam.

Chin,
6
13